Kam Yee Yoon[1,2]
Wen Siang Tan[2,3]
Beng Ti Tey[4]
Khai Wooi Lee[5]
Kok Lian Ho[1]

[1]Department of Pathology, Faculty of Medicine and Health Sciences, Universiti Putra Malaysia, Selangor, Malaysia
[2]Institute of Bioscience, Universiti Putra Malaysia, Selangor, Malaysia
[3]Department of Microbiology, Faculty of Biotechnology and Biomolecular Sciences, Universiti Putra Malaysia, Selangor, Malaysia
[4]Chemical Engineering Discipline, School of Engineering, Monash University, Sunway Campus, Jalan Lagoon Selatan, Bandar Sunway, Selangor, Malaysia
[5]School of Biosciences, Division of Medicine, Pharmacy and Health Sciences, Taylor's University Lakeside Campus, Malaysia

Received May 3, 2012
Revised September 9, 2012
Accepted September 12, 2012

Research Article

Native agarose gel electrophoresis and electroelution: A fast and cost-effective method to separate the small and large hepatitis B capsids

Hepatitis B core antigen (HBcAg) expressed in *Escherichia coli* is able to self-assemble into large and small capsids comprising 240 (triangulation number $T = 4$) and 180 (triangulation number $T = 3$) subunits, respectively. Conventionally, sucrose density gradient ultracentrifugation and SEC have been used to separate these capsids. However, good separation of the large and small particles with these methods is never achieved. In the present study, we employed a simple, fast, and cost-effective method to separate the $T = 3$ and $T = 4$ HBcAg capsids by using native agarose gel electrophoresis followed by an electroelution method (NAGE-EE). This is a direct, fast, and economic method for isolating the large and small HBcAg particles homogenously based on the hydrodynamic radius of the spherical particles. Dynamic light scattering analysis demonstrated that the $T = 3$ and $T = 4$ HBcAg capsids prepared using the NAGE-EE method are monodisperse with polydispersity values of ~15% and ~13%, respectively. ELISA proved that the antigenicity of the capsids was not affected in the purification process. Overall, NAGE-EE produced $T = 3$ and $T = 4$ capsids with a purity above 90%, and the recovery was 34% and 50%, respectively (total recovery of HBcAg is ~84%), and the operation time is 15 and 4 times lesser than that of the sucrose density gradient ultracentrifugation and SEC, respectively.

Keywords:
Electroelution / Hepatitis B core antigen / Homogenous sample / Native agarose gel electrophoresis
DOI 10.1002/elps.201200257

1 Introduction

Hepatitis B virus (HBV) infection is a major cause of chronic hepatitis, cirrhosis, and hepatocellular carcinoma, which claims about 600 000 lives per annum worldwide [1]. The viral envelope consists of three distinct but related hepatitis B surface antigens (HBsAg); namely long (L), medium (M), and short (S) polypeptides [2]. The inner nucleocapsid is surrounded by an outer envelope containing a 3.2 kb partially dsDNA molecule. The viral capsid is composed of multiple copies of hepatitis B core antigen (HBcAg) containing 183 residues with a molecular mass of ~21 kDa [3]. The C-terminal region of the HBcAg is highly rich in arginine and is believed to be involved in nucleic acid packaging [3].

HBcAg expressed in *Escherichia coli* self-assembles into particles of two sizes approximately 36 nm and 32 nm in diameter that morphologically similar to the capsids isolated from infected patients [4]. Cryoelectron microscopy revealed that the large and small particles are composed of 240 (triangulation number $T = 4$) and 180 (triangulation number $T = 3$) copies of HBcAg, respectively [5]. Removal of the arginine-rich C-terminus after residues 149 leads to a higher level of protein expression in *E. coli*, with predominantly $T = 4$ capsids, compared to the full-length HBcAg [6]. Image reconstructions of the $T = 4$ capsids derived from cryoelectron microscopy revealed the dimeric 4 α-helix-bundles on the surface of HBV capsids [7, 8]. The molecular details at atomic resolution were improved greatly through X-ray study, which solved the $T = 4$ capsid structure to a maximum resolution of 3.3 Å [9]. In contrast, the structure of $T = 3$ remained unsolved although the X-ray diffraction data were collected to 8 Å resolution [10].

The HBcAg expressed in *E. coli* forms virus-like particles (VLPs), which can be used as diagnostic reagents and drug delivery vehicles [11, 12]. HBV capsids are highly immunogenic which stimulate the production of B cells, T cells, and cytotoxic T cells in animals and human [13, 14]. The self-assembly capability of HBcAg can be manipulated to display foreign

Correspondence: Dr. Kok Lian Ho, Department of Pathology, Faculty of Medicine and Health Sciences, Universiti Putra Malaysia, 43400 UPM Serdang, Selangor, Malaysia
E-mail: klho@medic.upm.edu.my
Fax: +603-8941-2787

Abbreviations: HBcAg, hepatitis B core antigen; **HBV**, hepatitis B virus; **NAGE**, native agarose gel electrophoresis; **NAGE-EE**, NAGE and electroelution; **VLP**, virus-like particle

Colour Online: See the article online to view Fig. 1 in colour.

epitopes on the VLP. These epitopes derived from foot-and-mouth disease virus, plasmodium *spp*., influenza virus, and anthrax protective antigen [15–19]. Due to its potential applications in the development of multicomponent vaccines and diagnostic reagents, hence it is of importance to establish an effective method to purify and to separate the HBcAg large and small particles.

Conventionally, purification of HBcAg capsids is achieved by sucrose density gradient ultracentrifugation [10, 20]. However, multiple rounds of ultracentrifugation are required in order to achieve considerably pure $T = 3$ and $T = 4$ HBcAg particles. Gel filtration chromatography using HPLC was performed by [21] but the protein sample was found to be polydisperse due to the presence of $T = 3$ and $T = 4$ capsids. Other methods that have been established include immobilized metal affinity chromatography [22] and anion exchange expanded bed adsorption chromatography [23]. Generally, these methods are time consuming, laborious, and usually involved sophisticated instruments. Moreover, clear separation of the large and small particles with these methods have yet to be achieved despite the needs of successive rounds of ultracentrifugation and gel filtration chromatography.

In this study, an electrophoresis method was established with a high resolving power to purify and separate the large and small HBcAg particles into two homogenous populations. To achieve this goal, a combination of native agarose gel electrophoresis and electroelution (NAGE-EE) was employed to isolate $T = 3$ and $T = 4$ HBcAg capsids without involving advanced instrumentation. This newly established method reduces the time spent and experimental steps involved in the purification of HBcAg particles. To date, NAGE-EE system has not been reported to resolve the large and small HBcAg particles although it has been used widely in the separation of large protein complexes, nucleic acids, bacteriophages, and related capsids [24–26].

2 Materials and methods

2.1 Preparation of crude lysate

E. coli strain W311OIQ harboring the plasmid pR1–11E [27], which encodes the truncated HBcAg was cultured in Luria Bertani medium containing 100 μg/mL ampicillin. Production of HBcAg was induced by adding IPTG (0.5 mM) when the OD_{600} reached 0.8–1.0 and the incubation was continued for 16 h. The cells were harvested by centrifugation at 3750 × *g* (Avanti JLA-16.250; Beckman Coulter, USA) for 20 min at 4°C. The cell pellet was resuspended in 50 mM of Tris-HCl (pH 8.0) buffer. The cells were then lysed by adding lysozyme (0.2 μg/mL) supplemented with DNase 1 (15 μg/mL) and $MgCl_2$ (4 mM) at room temperature (25°C) for 2 h and followed by ultrasonication for 10 min with 20 s intervals in between pulses [28]. The cell debris was pelleted by centrifugation at 30 000 × *g* at 4°C for 20 min. Clarified lysate was used as crude lysate for subsequent purification process.

2.2 Ammonium sulfate precipitation

Ammonium sulfate was added slowly into the clarified lysate to obtain 35% saturation with continuous stirring on ice for 2 h. Precipitated proteins were recovered by centrifugation at 18 000 × *g* at 4°C for 30 min. The pellet containing the HBcAg was resuspended in 50 mM Tris-HCl, 100 mM NaCl (pH 8) buffer, and dialyzed against the same buffer with two changes.

2.3 Sucrose density gradient ultracentrifugation

The dialyzed HBcAg protein (200 μL) was layered on top of sucrose gradient (8–40%) solution and centrifuged at 150 000 × *g* at 4°C for 5 h [6]. The gradient solution was fractionated into 24 microcentrifuge tubes (500 μL each). The proteins in the fractions were analyzed by SDS-PAGE and quantified by using the Bradford assay [29]. The earlier and later sedimenting fractions of HBcAg were pooled separately and dialyzed against 50 mM Tris-HCl, 100 mM NaCl (pH 8) for overnight.

2.4 Size exclusion chromatography (SEC)

SEC was performed with Sephacryl-500 (GE Healthcare) packed in an XK 16/100 column (Amersham, USA) that attached to a fast protein liquid chromatography (FPLC) system (Akta Purifier; GE Healthcare, Sweden). The clarified lysate (2 mL) was loaded onto the column that had been equilibrated with 50 mM Tris-HCl, 100 mM NaCl (pH 8). Proteins were resolved using a flow rate of 0.5 mL/min and fractions were collected with a fraction collector (Frac-950). Based on the chromatogram, the fractions containing the large and small HBcAg particles were pooled separately.

2.5 NAGE

NAGE was performed by using 1.5% w/v agarose gel with a dimension of 20.5 cm × 20.5 cm and 2 cm thick, casted on a Maxicell electrophoresis set (EC360m, St. Petersburg, Floride, USA). The crude lysate without ammonium sulfate cut was loaded into a combined well and electrophoresed in 0.5 X TBE buffer (90 mM Tris-borate, 2 mM EDTA, pH 8.3) at 80 V for 3.5 h at room temperature. Due to the large amount of loaded HBcAg, the migration of the HBcAg particles could be observed by the naked eye without staining.

2.6 Electroelution of proteins

The protein bands corresponding to the large and small HBcAg particles were excised from the agarose gel using a sharp scalpel. The gel slices were transferred to a dialysis

tube filled with 0.5× TBE buffer. The dialysis tubes containing the gel slice were electrophoresed for 60 min using the same condition. The gel slices were removed and the sample was dialyzed in 50 mM Tris-HCl, 100 mM (pH 8) for 5 h at 4°C.

2.7 SDS-PAGE

All samples were analyzed with SDS-PAGE as described by Laemmli [30]. The protein samples were separated on 15% w/v resolving polyacrylamide gel at 16 mV using a Mini-Protean 3 electrophoresis set (Bio-Rad, USA). The gel was then stained with CBB-R250 (CBB-R250) and destained with destaining solution containing 40% v/v methanol and 10% v/v acetic acid.

2.8 Quantitation of HBcAg

Quantitation of HBcAg was performed as described previously by Ng et al. [31]. The amount of HBcAg in the samples was determined using the Quantity One® Quantitation software (Gel Doc; Bio-Rad) and calculated based on the relative quantity of the HBcAg band separated on the SDS-polyacrylamide gel against the amount of total protein obtained from the Bradford assay.

2.9 Silver staining

Polyacrylamide gel was fixed with 40% v/v ethanol and 10% v/v acetic acid for 30 min. The gel was washed several times with dH_2O before adding 0.02% w/v sodium thiosulfate and incubated for 2 min. Then, the gel was washed three times with dH_2O until the yellow color disappeared. The silver reagent; 0.1% w/v silver nitrate was added and incubated for 30 min. Finally, the color development was performed by adding developer containing 2.5% v/w sodium carbonate and 0.04% v/v formalin (BioRad). The reaction was stopped by adding 5% v/v acetic acid.

2.10 Western blot analysis

The separated proteins on the polyacrylamide gel were transferred onto an NC membrane using a semidry blotter (Trans-Blot® SD, BioRad). The NC membrane was then blocked with milk diluent (KPL, USA; 1:10 dilutions) for 1 h at room temperature. After three times of washing with TBS-T (50 mM Tris-HCl, pH 7.6; 150 mM NaCl; 0.1% Tween 20), the NC membrane was incubated with anti-HBcAg mAb (mAb C1–5; Chemicon International, Temecula, CA, USA) for 1 h at room temperature. Afterwards, the NC membrane was washed with TBS-T and incubated with alkaline phosphatase conjugated goat anti-mouse antibody (1:5000 dilutions) for 1 h at room temperature. The immunoblotted bands were developed by adding 5-bromo-4-chloro-3-indolyl phosphate/nitro blue tetrazolium (BCIP/NBT) in alkaline phosphatase buffer [100 mM Tris-HCl (pH 9.5), 100 mM NaCl, 5 mM $MgCl_2$]. Color development was terminated by incubating the NC membrane with dH_2O and the developed membrane was dried at room temperature.

2.11 ELISA

Microtiter plate wells were coated with the purified HBcAg particles (0–1000 ng) for 16 h at 4°C. The coated wells were washed with TBS-T buffer, blocked with milk diluents for 2 h at room temperature. The wells were then washed with TBS-T before adding anti-HBcAg mAb for 1 h at room temperature. Next, the wells were washed three times with TBS-T and incubated with anti-mouse IgG (1:5000 dilutions) at room temperature for 1 h. After washing, substrate (0.01 g p-NPP and 10 mL diethanolamine (DEA) buffer; pH 8; 200 μL) was added into the wells and incubated at room temperature for 10–15 min. The reactions were terminated by adding NaOH (3N; 50 μL) and absorbance at 405 nm was measured by using a microtiter plate reader (Bio-Tek, Winooski, USA).

2.12 Dynamic light scattering analysis

The purified large and small particles of HBcAg (0.25 mg/mL) were loaded into a quartz cuvette cell through syringe filters with 0.02 μm molecular cut-off. The sample cell was passed through a light from a near infrared semiconductor laser (825 nm wavelength), at 35 mW power (Dyna Pro – 801™, Protein Solutions Ltd. High Wycombe, UK). Each measurement is recorded as an average of 20 readings. The scattered light at 90° angle was detected and recorded by an avalanche photo diode detector at 4°C. The translational diffusion coefficient of a particle in solution, D_T was derived. The hydrodynamic radius, R_H was calculated from D_T using the Stokes Einstein equation $D_T = kT/6\pi\eta R_H$ and $R_H = k_B T/6\pi\eta D_T$, where k_B is the Boltzmann constant, T is absolute temperature in Kelvin, and η is the solvent viscosity. The viscosity of the water is $\eta = 1.019 \times 10^{-3}$ Nsm^{-2}. The percentage of polydispersity reported in the study is derived from polydispersity index, which is used to describe the SD of the spread of particle sizes based on the average R_H measured [32]. Monodisperse sample typically has a polydispersity value that is less than 20% of the mean value of R_H. Polydispersity value and R_H of the sample were calculated by using the Dynamic V5 software (Proterion, USA).

2.13 Transmission electron microscopic analysis

Purified HBcAg particles (15 μL, 0.25 mg/mL) were absorbed onto carbon-coated grids (200 mesh) and negatively stained with freshly prepared 2% uranyl acetate for 5 min. The grids were observed under a transmission electron microscope

(Hitachi-700) and micrographs were taken at appropriate magnifications.

2.14 Calculations

Purity is defined as the amount of purified HBcAg particles divided by the amount of total protein in the sample.

$$\text{Purity (\%)} = \frac{\text{Amount of HBcAg}}{\text{Amount of total protein}} \times 100\% \quad (1)$$

The purification factor is calculated by the ratio of the purity of HBcAg particles recovered to the purity of HBcAg particles in the crude lysate.

$$\text{Purification factor} = \frac{\text{Purity of HBcAg}}{\text{Purity of HBcAg in the crude lysate}} \quad (2)$$

Recovery is calculated as a percentage of recovered HBcAg capsids from the initial amount of HBcAg in the crude lysate.

$$\text{Recovery (\%)} = \frac{\text{Amount of recovered HBcAg}}{\text{Initial amount of HBcAg}} \times 100\% \quad (3)$$

3 Results and discussion

3.1 Purification of HBcAg particles using sucrose density gradient ultracentrifugation and SEC

HBV capsids with two different sizes have been purified by using density gradient centrifugation, SEC, and affinity absorption chromatography [10, 21, 33, 34]. These methods are able to purify the capsids to high levels of purity based on SDS-PAGE or mass spectrometric analysis but cannot exclusively fractionate the HBV capsids into different populations within a short period. Cryoelectron microscopy revealed that the surface properties of the large and small HBcAg capsids are similar except their structural geometry [5], indicating that most outer surface characteristics including the protein antigenicity are invariable between these capsids. Thus, absolute separation of $T = 3$ and $T = 4$ HBcAg capsids is not always performed comprehensively because a mixture of the large and small HBcAg capsids would not affect the results of many biophysical assays. However, in the areas of structural biology (such as protein X-ray crystallography, cryo-electron microscopy, and neutron diffraction) purity and homogeneity are the most crucial factors, which ensure the success of these studies. In most cases, the full-length and truncated HBcAg assembled predominantly into large HBcAg capsids [6]. The high ratio of large to small HBcAg particles and the small geometrical variation (only ~2 nm differ in hydrodynamic radius) among these particles impose difficulty in isolating the $T = 3$ capsids from the mixture of these particles using the conventional methods. Conversely, to maximize the homogeneity of $T = 4$ capsids, considerable amount of the large particles need to be omitted as a preference to avoid cross-contamination from $T = 3$ capsids in order to enhance the homogeneity of the samples.

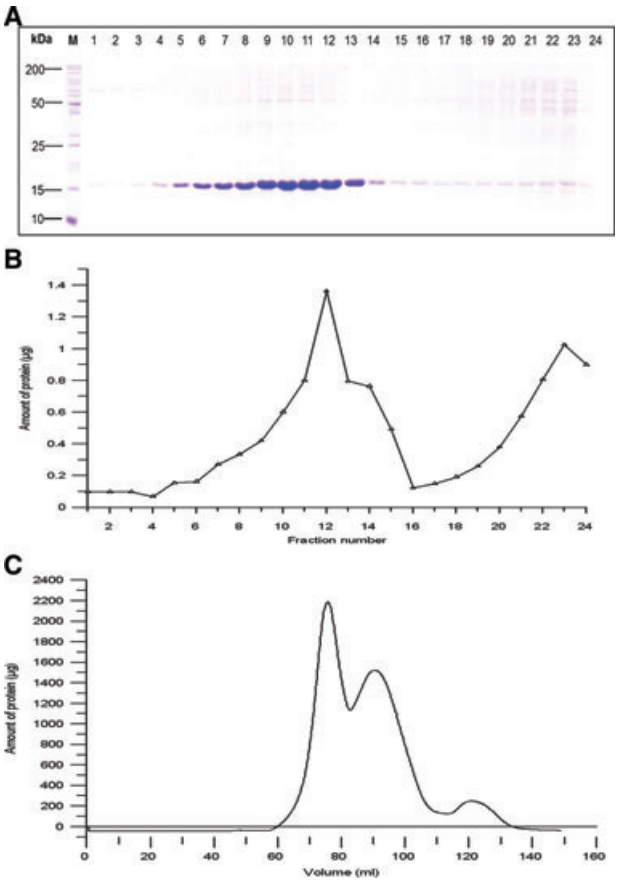

Figure 1. Sucrose density gradient ultracentrifugation and SEC. (A) SDS-PAGE of the migration profile of HBcAg particles from 8% to 40% sucrose density gradient. (B) The migration profile of HBcAg particles from 8% to 40% sucrose density gradient ultracentrifugation determined by the Bradford assay. (C) Chromatograph of the large and small HBcAg particles fractionated by S-500 SEC on an FPLC system.

In this study, the truncated HBcAg was highly expressed as soluble proteins in W3110IQ cells and the crude lysate was clarified by ammonium sulfate precipitation with 35% w/v saturation prior to sucrose density gradient ultracentrifugation. Fractionated samples were analyzed by SDS-PAGE and the protein concentration was determined by using the Bradford assay (Fig. 1). A dominant band of approximately 17 kDa that corresponds to the truncated HBcAg was observed in fractions 4 to 14 (Fig. 1A). The migration profile of the HBcAg capsids showed two peaks which overlapped significantly from fractions 10 to 15 (Fig. 1B). The large and small particles were separated by combining the fractions from the first half of the major peak (fractions 7 to 11) and the second half of the minor peak (fractions 14 to 16), respectively. The middle fractions were excluded from these populations in order to minimize the contamination of the heavily overlapped

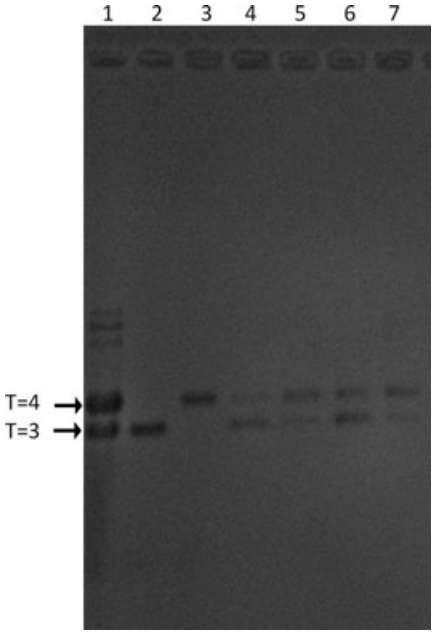

Figure 2. NAGE. Large and small HBcAg particles purified with the NAGE-EE, sucrose density gradient ultracentrifugation, and SEC protocols were separated on 1.5% native agarose gel. The agarose gel was stained with CBB. Lane 1 contains 200 μg of the total protein in crude lysate, fractionation of HBcAg using NAGE-EE protocol for $T = 3$ and $T = 4$ are shown in lanes 2 and 3, respectively. $T = 3$ and $T = 4$ preparations by sucrose density gradient ultracentrifugation are shown in lanes 4 and 5, respectively, and $T = 3$ and $T = 4$ preparations using SEC are shown in lanes 6 and 7, respectively. The amount of protein loaded in lanes 2–7 is 50 μg.

regions that contained a mixture of $T = 4$ and $T = 3$ capsids. However, native agarose gel electrophoresis (NAGE) analysis (Fig. 2, lanes 4 and 5) showed that this strategy could not separate the large and small HBcAg particles into two distinct populations as these particles were present in both samples. This observation was supported by electron microscopic analysis, which demonstrates that $T = 4$ and $T = 3$ capsids with a diameter of approximately 36 nm and 32 nm, respectively, were still observed in both preparations (Fig. 3A and D).

In the SEC, the clarified lysate resolved in Sephacryl-500 HR (Pharmacia) resin that had been packed in an XK 16/100 column (GE Healthcare) with a diameter and length of 16 mm and 100 cm, respectively. Sephacryl-500 resin with an exclusion limit of approximately 100 nm in radius [35] is an appropriate matrix to purify HBcAg particles with radii of 16–18 nm. Protein separation profile of the HBcAg particles by SEC showed two overlapping peaks between elution volume 60 mL and 110 mL (Fig. 1C). Similar to the sucrose gradient ultracentrifugation, SDS-PAGE, and electron microscopy indicated that the large and small particles of HBcAg were not well separated using this method. As described, similar strategy was attempted to separate the large and small HBcAg particles, however, NAGE and electron microscopic examinations revealed that the pooled $T = 4$ and $T = 3$ HBcAg particles were contaminated with the large and small capsids, respectively (Fig. 2, lanes 6 and 7 and Fig. 3B and E).

The results demonstrate that a single round sucrose gradient density ultracentrifugation or SEC could not separate $T = 3$ and $T = 4$ particles exclusively. To improve the HBcAg particles separation, a second round of sucrose gradient density ultracentrifugation and SEC were carried out using populated mixture of $T = 4$ and $T = 3$ HBcAg capsids. This approach enhanced the protein purity to approximately 90% but the sample remained heterogeneous, as both $T = 3$ and $T = 4$ HBcAg capsids coexist in each populated sample. In both methods, the final yield of HBcAg reduced dramatically as the strategy used to pool $T = 3$ and $T = 4$ capsids omitted the HBcAg particles that lay within the overlapping regions of the protein migration profiles.

3.2 Purification of HBcAg particles by NAGE

Since purification of HBcAg particles using sucrose density gradient ultracentrifugation and SEC could not separate the large and small particles homogenously, NAGE was employed to separate these two particles based on their sizes and overall charges. In this simple method, the crude lysate without ammonium sulfate cut (total protein loaded 200 μg) was electrophoresed in a buffer without reducing agent at room temperature. The large and small HBcAg particles can be exclusively separated by the gel into two discrete dominant bands, with the upper and lower bands corresponding to large and small capsids, respectively (Fig. 2, lane 1). The distance between these two bands was approximately 0.5 cm and this allowed the protein bands to be excised and transferred into two dialysis tubes. The HBcAg capsids were electroeluted from the gel slices using the same electrophoresis condition. The recovered HBcAg (50 μg) were analyzed with an additional run of NAGE in order to confirm the homogeneity of the fractionated samples. Figure 2 (lanes 2 and 3) shows a single protein band that corresponds well with the small and large HBcAg capsids, respectively, as they comigrated with the dominant bands in the crude lysate. SDS-PAGE analysis revealed an intense 17 kDa band in the lanes that contain HBcAg from $T = 3$ and $T = 4$ HBcAg capsids preparations (Fig. 4A, lanes 3 and 4, respectively) as observed in lanes containing the crude and ammonium sulfate clarified lysates (Fig. 4A, lanes 1 and 2, respectively). The results demonstrate that the NAGE-EE is capable to separate the $T = 3$ and $T = 4$ HBcAg capsids.

HBV capsids fractionated by NAGE were analyzed with transmission electron microscopy. As shown in the micrographs (Fig. 3C and F), negatively stained large and small HBV capsids can be seen as spiky spherical shells with diameter of ~36 nm and ~32 nm, respectively. However, electron microscopy alone is insufficient to discriminate accurately the sizes of the particles with similar morphology due to the possibility of flattening and shrinkage effects that resulted from negative staining with uranyl acetate as observed in electron microscopic analysis of bacteriophage T7 particles [36]. To

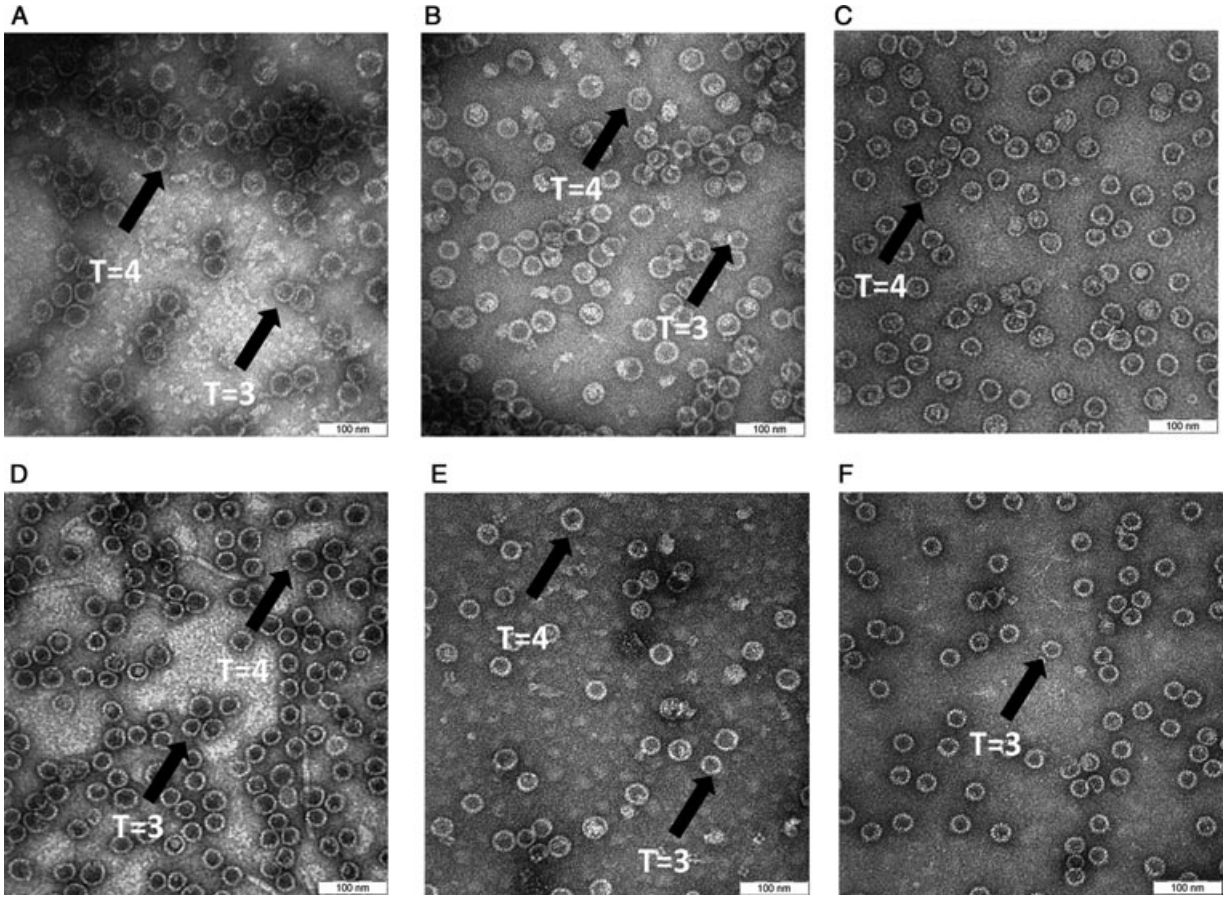

Figure 3. Electron micrographs of HBcAg particles. Recovered HBcAg particles were dialyzed and negatively stained with 2% uranyl acetate. Electron micrographs of $T = 4$ preparation by (A) sucrose density gradient ultracentrifugation, (B) SEC, and (C) NAGE-EE. Electron micrographs of $T = 3$ preparation by (D) sucrose density gradient ultracentrifugation, (E) SEC, and (F) NAGE-EE. The $T = 4$ and $T = 3$ HBcAg particles with diameters approximately 36 nm and 32 nm, respectively, are indicated by arrows.

rule out these distortion effects, dynamic light scattering was performed to determine the hydrodynamic radius and the polydispersity of the recovered HBcAg capsids. The radius of the small and large HBcAg particles was measured 15.5 ± 0.6 nm and 18.4 ± 0.3 nm, respectively, which is in good accord with that reported by Tan et al. [6]. The radius of the large particle (17.5 nm) is similar with that determined by X-ray crystallography [9, 37].

Light scattering measurements of the NAGE recovered HBcAg capsids showed a monodisperse size distribution in solution as indicated by low polydispersity values of ~15% and 13%, for the small and large HBcAg capsids, respectively (Table 1). In contrast, HBV capsids recovered from sucrose gradient density ultracentrifugation and SEC showed a higher polydispersity in solution with values above 28% (Table 1). The major factor that increased the polydispersity value of the recovered capsids using sucrose gradient density ultracentrifugation and SEC is likely due to the presence of both capsids with different sizes in each preparation which is consistent with NAGE analysis (Fig. 2, lanes 4 to 7). Unspecific large protein aggregates were unlikely to present as all the samples were filtered prior to light scattering analysis.

In nonreducing agarose gel electrophoresis, migration of macromolecules depends on the surface characteristics and the molecular dimension of the macromolecules [26]. The electrophoretic mobility of the macromolecules is affected by the percentage of agarose gel, in which, viral particles are fractionated primarily by average surface charge rather than the particle radius in a diluted agarose gel and the opposite is true if the gel percentage is raised when the effective pore size is large enough to permit particle migration [38]. This was demonstrated by using a 2D agarose gel with a lower agarose percentage in the first dimensional electrophoresis and a higher percentage in the second dimensional electrophoresis when the gel field is rotated at 90° [24, 26]. Nanoparticles that were successfully fractionated with this 2DE include conjugated *Haemophilus influenza* vaccines, bacteriophages T7/T3, and related capsids [24, 26]. When the percentage of agarose gel increases, the "sieving effects" that caused by the presence of fibers in the solidified gel become a significant factor that decreases the motion of the spherical particles in the gel matrices by reducing the effective pore size that permits the particle migration [26]. The spherical particles are sieveable through the gel as long

Table 1. Dynamic light scattering analysis of recovered HBcAg capsids

Method	Sucrose density gradient ultracentrifugation		Native agarose gel electrophoresis		Gel filtration	
Triangulation number	$T = 3$	$T = 4$	$T = 3$	$T = 4$	$T = 3$	$T = 4$
Hydrodynamic radius (nm)	16.0 ± 0.8	18.0 ± 1.7	15.5 ± 0.6	18.4 ± 0.3	15.9 ± 0.8	17.6 ± 0.1
Polydispersity (%)	28.7 ± 2.1	35.5 ± 3.4	14.8 ± 1.6	13.1 ± 1.7	28.5 ± 2.1	28.7 ± 0.9

as the effective pore size is larger than the diameter of the spheres. A quantitative model of these effects is reported in Griess et al. [39].

Monomers of HBcAg assemble to yield particles with two different sizes that are similar in appearance, but distinguishable in geometrical symmetries [5]. X-ray studies showed that the asymmetric unit of the capsids is the HBcAg dimer, which forms the spikes that protrude outward from the core of the shells [9, 37]. Similarities of the surface characteristics suggest that both the large and small HBcAg particles have similar average surface charge but differ in capsid diameter. In this study, the HBcAg capsids were fractionated in a 1.5% nonreducing agarose gel, suggesting that the diameter of the HBcAg capsids is smaller than the effective pore size of the agarose gel but is large enough to be sieved through the agarose fibers at this percentage. The sieving effect functions as a retardation force in limiting the rate of migration, in which, it is spherical radius dependence at a given agarose percentage. If diluted agarose gel is used, the sieving effect becomes too small to discriminate the electromobility of the large and small HBcAg capsids that only differ about 2 nm in radius. The result indicates that HBcAg capsids with a diameter of ~32 nm or ~36 nm were indeed fractionated mainly by hydrodynamic radius of the particles in a 1.5% agarose gel and the average surface charge of both particles provides electrostatic forces that most likely with the same capacity to move the capsids toward the anode.

Subsequently, the quality of the HBcAg capsids that recovered from NAGE by various methods was studied. As shown in electron micrographs (Fig. 3), all the recovered HBcAg capsids that gave rise to intact spherical particles are morphologically similar to those recovered from sucrose density gradient ultracentrifugation and SEC. The result indicates that the morphology of the assembled viral particles was stable during the NAGE, although this method could not discriminate the diameter of the particles precisely. SDS-PAGE analysis using the recovered capsids from NAGE revealed a discrete protein band of approximately 17 kDa without any sign of degradation as compared with those purified using the other two methods (Fig. 4A, lanes 5–8). This demonstrates that the HBcAg monomer is not damaged during NAGE although degradation products were observed in NAGE purification of the capsid II of bacteriophage T7 [40]. In fact, protein crystals of the HBcAg large capsids were reproducible by using the NAGE recovered $T = 4$ HBcAg with the crystallization condition described by Tan et al. [37] (data not shown). The antigenicity of the HBcAg capsids recovered from NAGE-EE, sucrose density gradient ultracentrifugation, and SEC was studied with ELISA. The results showed that the capsids recovered from all the three purification methods reacted strongly (A_{405} above 0.5 for 50 ng of coated HBcAg, Fig. 5) with the anti-HBcAg mAb that interacts with the immunodominant region of the HBcAg located at the tip of the spikes. This indicates that the antigenicity of the

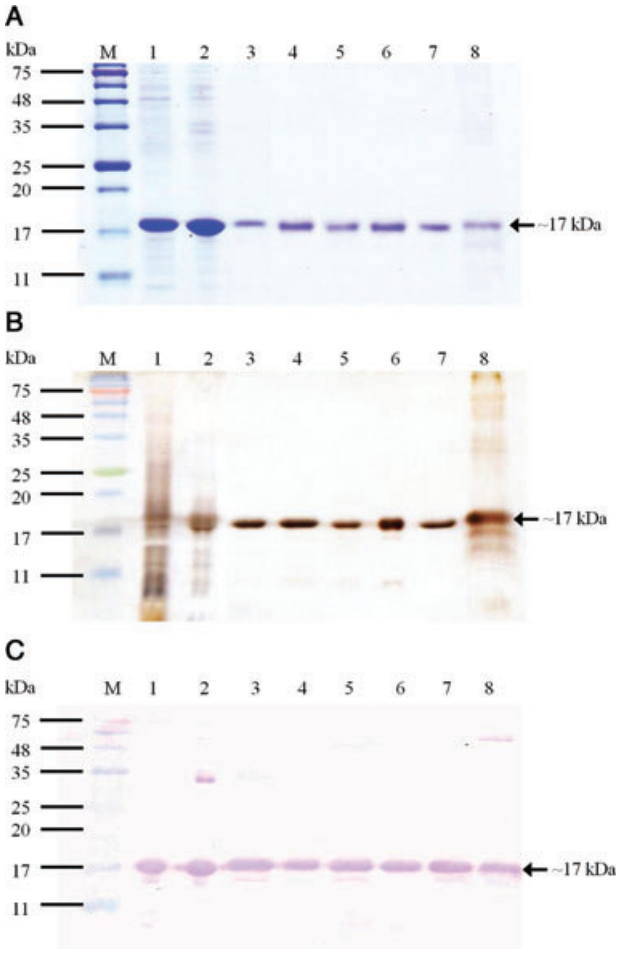

Figure 4. SDS-PAGE analysis, silver staining, and Western blot. (A) SDS-polyacrylamide gel stained with CBB, (B) SDS-polyacrylamide gel stained with silver nitrate, and (C) immune-blotting against anti-HBcAg mAb. Lane M, molecular mass markers in kDa; lane 1, the crude lysate (10 g); lane 2, HBcAg after ammonium sulfate precipitation (10 μg); lanes 3 and 4, $T = 4$ and $T = 3$, respectively, from NAGE-EE; lanes 5 and 6, $T = 4$ and $T = 3$, respectively, from sucrose density gradient ultracentrifugation and lanes 7 and 8, $T = 4$ and $T = 3$, respectively, from SEC. Same amount of protein (2 g) was loaded in lane 3 to lane 8.

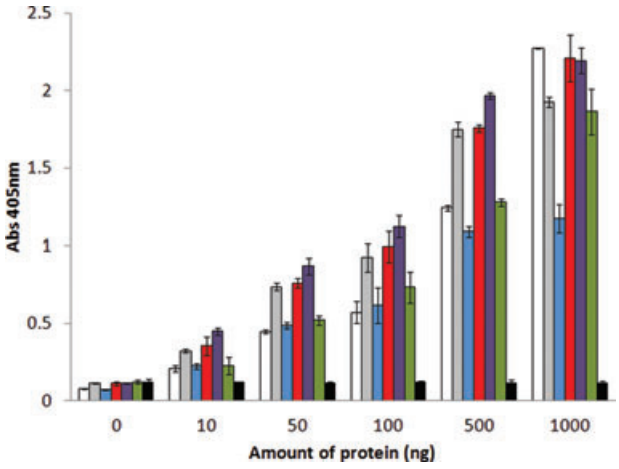

Figure 5. ELISA analysis. The antigenicity of HBcAg particles was measured as absorbance at 405 nm against different amount of HBcAg (0–1000 ng) coated on the wells. The $T = 4$ and $T = 3$ HBcAg capsids fractionated by sucrose density gradient ultracentrifugation are represented by white and gray bars, respectively. The $T = 4$ and $T = 3$ HBcAg capsids fractionated by SEC are shown by blue and red bars, respectively, whereas the purple and green bars represent the $T = 4$ and $T = 3$ HBcAg capsids fractionated by NAGE-EE, and negative control is indicated by black bar.

purified capsids is not affected by the NAGE as well as the other two methods. These demonstrated that the recovered HBcAg capsids are stable, intact, and biologically active.

To determine the purity and specificity of the proteins recovered from all the three purification methods, the polyacrylamide gel was stained with silver nitrate (Fig. 4B) and immunoblotted with the anti-HBcAg mAb (Fig. 4C). With sensitivity of ~30 to 100 times higher than CBB [41], silver staining enhanced the intensity of the protein bands in the polyarcylamide gel compared to that of CBB stained gel. Impurity was detected in the $T = 3$ capsids purified with sucrose density gradient ultracentrifugation and SEC (Fig. 4B, lanes 6 and 8). This is most likely due to the fact that the host proteins, which overlapped the tail of the $T = 3$ profile were present in the $T = 3$ preparation using both methods. Interestingly, only a single sharp band of ~17 kDa was detected for proteins that recovered from NAGE-EE. Western blotting detected a dominant band of ~17 kDa. In addition to this major band, a protein band ~34 kDa, which is believed to be the dimer of HBcAg, is also present in the ammonium sulfate cut preparation. Overall, the purities of the HBcAg capsids that recovered from these methods are equally high and satisfactory either determined with CBB staining or silver staining. Western blotting proved that the dominant bands in the SDS-polyacrylamide gel are indeed the HBcAg.

3.3 Comparison of sucrose density gradient ultracentrifugation, SEC, and NAGE-EE

Table 2 summarizes the purification of HBcAg particles using sucrose density gradient ultracentrifugation, SEC, and NAGE-EE. All these methods are able to purify HBcAg to high purity (above 90%), except the $T = 3$ preparation from SEC, from the initial purity of ~16% (crude lysate) as calculated using Eq. (1) as described in Section 2. However, the value of purity could not represent the homogeneity of the samples as cross-contamination between these capsids is undetectable. Based on Eq. (3), the initial amount of HBcAg in the crude lysate was quantified from SDS-polyacrylamide gel and the recovered HBcAg was determined by the Bradford assay. The results demonstrated that the total recovery in NAGE-EE approach is ~20% higher compared to that of sucrose density ultracentrifugation and SEC. Individually, the large and small HBcAg capsids recovered from NAGE-EE method are ~50% and ~34%, respectively, of the total HBcAg (sum of $T = 3$ and $T = 4$) in the cell lysate.

The high recovery of HBcAg capsids in NAGE-EE could, at least partially, attribute to the unique characteristics of the particles. It is by nature that the HBcAg capsids exist as spherical particles and assembled from a single species of protein. Dimer clustering of $T = 3$ and $T = 4$ quasi-equivalence produces two shells with distinct diameter [5], which could be fractionated efficiently in the agarose gel depending on agarose percentage. In contrast, other systems such as bacteriophage T7 and its related capsids are composed of multiple proteins, with different capsid thickness and the availability of tails [42]. These rather amorphous characteristics could potentially influence the migration of the capsids in the nonreducing agarose gel. Concerning the shape of VLPs, NAGE-EE could serve as a preferred method to purify spherical capsids. The purification factors (Table 2) that are calculated based on the ratio of purity of HBcAg in the recovered $T = 3$ and $T = 4$ capsids and the purity of the initial total HBcAg in the crude lysate are less significant compared to that of polydispersity values, which indicate the homogeneity of the samples. Out of these methods, only NAGE-EE was able to separate the HBcAg capsids into monodisperse populations (Table 1).

In this study, the simplicity and efficiency of NAGE-EE were demonstrated by its relatively less laborious procedure compared to the other two methods. This is partly because NAGE-EE allows direct purification of HBcAg particles from the total protein in crude lysate without ammonium sulfate precipitation. Hence, a process to remove ammonium sulfate via dialysis or desalting column chromatography was not required. By manipulating the thickness and the size of the slab agarose gel, large quantity of crude lysate can be loaded and electrophoresed. Figure 6 shows that high quantity of protein in crude lysate (~21 mg) was fractionated in a 1.5% agarose gel and the recovered HBcAg capsids (~10 mg each in lanes 2 and 3) were analyzed under the same experimental condition. HBV capsids migration was monitored by naked eyes without staining and the usage of chemical reagents such as CBB, methanol, and acetic acid in preparing staining and destaining solutions are not required. The well-separated intense protein bands can then be excised directly from the agarose gel without the need of visual aids. The simple application of the NAGE-EE suggests that this is a convenient

Table 2. Comparison between NAGE, SEC, and sucrose density gradient ultracentrifugation for the purification and fractionation of HBcAg capsids

Type of method	Amount of HBcAg (mg)		Purity (%)		Purification factor[a)]		Recovery (%)		Operation time (h)
Triangulation number	$T=3$	$T=4$	$T=3$	$T=4$	$T=3$	$T=4$	$T=3$	$T=4$	–
Initial crude lysate	7 (43)[b)]		16.3		1.0	1.0	–	–	–
NAGE-EE	2.4	3.5	91	92	5.6	5.6	34.3	50.0	4.0
Sucrose gradient ultracentrifugation	2.1	2.3	92	94	5.6	5.8	30.0	32.9	48–72
SEC	1.4	3.3	85	91	5.2	5.6	20.0	47.1	12–15

a) Purification factors expressed in this column are the ratio of the purity of $T=3$ or $T=4$ for each method to the purity of the total HBcAg (sum of $T=3$ and $T=4$) in the crude lysate.
b) Total protein in the crude lysate.

extraction method for HBV capsids and other spherical viral particles.

As demonstrated by Zlotnick et al. [43], the amount of $T=3$ HBcAg particles produced in *E. coli* harboring a truncated *HBcAg* gene is less than 40%. Hence, loss of $T=3$ HBcAg capsids in the conventional multistep purification protocols could further reduce the final yield. In contrast, NAGE-EE allows higher recovery of $T=3$ particles by not intentionally excluded considerable amount of this capsid for the homogeneity of $T=4$ particles as practiced in the other methods. This advantage is particularly important in isolating $T=3$ HBcAg particles in order to compensate for the lower levels of small HBcAg capsid assembly compared to that of the large counterparts. As a result, purification and separation of HBcAg particles with two different sizes using NAGE-EE technique is much favorable. Overall, the results suggest that purification and separation of $T=3$ and $T=4$ HBcAg particles using NAGE-EE can serve as a simple two-step purification method: separation and elution under the same experimental conditions. Multiple rounds of electrophoresis are not required as a single round of NAGE-EE is sufficient to separate $T=3$ and $T=4$ HBcAg capsids into two different populations. Experimental steps in NAGE-EE with crude lysate as a starting material were completed within 4 h. In contrast, sucrose density gradient ultracentrifugation required 2–3 days to complete the purification steps. This exceptional long procedure could expose the protein for proteolytic cleavage and some functional destruction [44]. Although the SEC could reduce the sample exposure time to around 6 h, the pre- and post-run buffer equilibrium and washing steps, however, increase the time spent several folds.

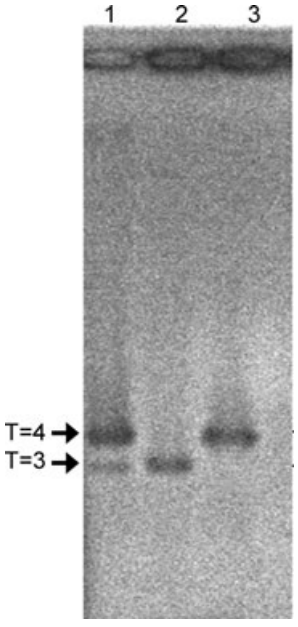

Figure 6. Electroelution of HBcAg particles. The crude lysate of HBcAg particles were shown in lane 1 (~21 mg of total protein). Lanes 2 and 3 are $T=3$ and $T=4$ particles, respectively (~10 mg of HBcAg in each lane), eluted from NAGE-EE.

4 Concluding remarks

We conclude that a simple, fast, and economic method has been established to purify and separate the large and small HBcAg capsids homogenously by using nonreducing agarose gel electrophoresis. This simple method can separate the $T=4$ and $T=3$ HBcAg particles within a shorter time and the samples were demonstrated to be monodisperse in solution as indicated by dynamic light scattering analysis. Electron microscopic analysis and ELISA confirmed that the pre-assembled viral particles are stable in the short dual-electrophoresis protocol. Generally, NAGE-EE provides an ideal alternative method for purification of, particularly, spherical VLPs without compromising the quantity and quality of the samples.

This work was supported by the RUGS Grant (Project No. 05-01-09-0623RU) from Universiti Putra Malaysia and the FRGS Grant (Project No. 03-10-10-948FR) from the Ministry of Higher Education, Malaysia. Kam Yee Yoon is a Graduate Research Fellowship student and Khai Wooi Lee was supported by the Graduate Research Fellowship from Universiti Putra Malaysia.

The authors have declared no conflict of interest.

5 References

[1] Franco, E., Bagnato, B., Marino, M. G., Meleleo, C., Serino, L., Zaratti, L., *World J. Hepatol* 2012, *4*, 74–80.

[2] Heermann, K. H., Hagos, Y., Thomssen, R., *J. Virol. Methods* 1994, *50*, 43–57.

[3] Pasek, M., Goto, T., Gilbert, W., Zink, B., Schaller, H., MacKay, P., Leadbetter, G., Murray, K., *Nature* 1979, *282*, 575–579.

[4] Cohen, B. J., Richmond, J. E., *Nature* 1982, *296*, 677–679.

[5] Crowther, R. A., Kiselev, N. A., Bottcher, B., Berriman, J. A., Borisova, G. P., Ose, V., Pumpens, P., *Cell* 1994, *77*, 943–950.

[6] Tan, W. S., Dyson, M. R., Murray, K., *Biol. Chem*. 2003, *384*, 363–371.

[7] Bottcher, B., Wynne, S. A., Crowther, R. A., *Nature* 1997, *386*, 88–91.

[8] Conway, J. F., Cheng, N., Zlotnick, A., Wingfield, P. T., Stahl, S. J., Steven, A. C., *Nature* 1997, *386*, 91–94.

[9] Wynne, S. A., Crowther, R. A., Leslie, A. G., *Mol. Cell*. 1999, *3*, 771–780.

[10] Zlotnick, A., Palmer, I., Kaufman, J. D., Stahl, S. J., Steven, A. C., Wingfield, P. T., *Acta. Crystallogr. D Biol. Crystallogr*. 1999, *55*, 717–720.

[11] Lee, K. W., Tey, B. T., Ho, K. L., Tejo, B. A., Tan, W. S., *Mol. Pharmaceutics* 2012, *9*, 2415–2423.

[12] Lee, K. W., Tey, B. T., Ho, K. L., Tan, W. S., *J. Appl. Microbiol*. 2012, *112*, 119–131.

[13] Geldmacher, A., Skrastina, D., Petrovskis, I., Borisova, G., Berriman, J. A., Roseman, A. M., Crowther, R. A., Fischer, J., Musema, S., Gelderblom, H. R., Lundkvist, A., Renhofa, R., Ose, V., Kruger, D. H., Pumpens, P., Ulrich, R., *Virology* 2004, *323*, 108–119.

[14] Vanlandschoot, P., Cao, T., Leroux-Roels, G., *Antiviral Res*. 2003, *60*, 67–74.

[15] Schodel, F., Peterson, D., Hughes, J., Milich, D., *Int. Rev. Immunol*. 1994, *11*, 153–165.

[16] Zhang, Y. L., Guo, Y. J., Wang, K. Y., Lu, K., Li, K., Zhu, Y., Sun, S. H., *Scand. J. Immunol*. 2007, *65*, 320–328.

[17] Yin, Y., Zhang, J., Dong, D., Liu, S., Guo, Q., Song, X., Li, G., Fu, L., Xu, J., Chen, W., *Vaccine* 2008, *26*, 5814–5821.

[18] Ameiss, K., Ashraf, S., Kong, W., Pekosz, A., Wu, W. H., Milich, D., Billaud, J. N., Curtiss, R., 3rd, *Vaccine* 2010, *28*, 6704–6713.

[19] Yap, W. B., Tey, B. T., Alitheen, N. B., Tan, W. S., *J. Biosci. Bioeng*. 2012, *113*, 26–29.

[20] Dyson, M. R., Murray, K., *Proc. Natl. Acad. Sci. U S A* 1995, *92*, 2194–2198.

[21] Tang, K. F., Abdullah, M. P., Yusoff, K., Tan, W. S., *J. Med. Chem*. 2007, *50*, 5620–5626.

[22] Yap, W. B., Tey, B. T., Ng, M. Y., Ong, S. T., Tan, W. S., *J. Virol. Methods* 2009, *160*, 125–131.

[23] Ho, C. W., Tan, W. S., Chong, F. C., Ling, T. C., Tey, B. T., *J. Microbiol. Biotechnol*. 2009, *19*, 416–423.

[24] Tietz, D., *J. Chromatogr. A*. 2009, *1216*, 9028–9033.

[25] Stellwagen, N. C., *Electrophoresis* 2009, *30*, S188–S195.

[26] Serwer, P., in: Kurtböke, I. (Ed.), *Bacteriophages*, InTech, Rijeka 2012, pp. 39–54.

[27] Stewart, F. S., *PhD thesis*, University of Edinburgh, UK 1993.

[28] Ho, C. W., Tan, W. S., Kamaruddin, S., Ling, T. C., Tey, B. T., *Biotechnol. Appl. Biochem*. 2008, *50*, 49–59.

[29] Bradford, M. M., *Anal. Biochem*. 1976, *72*, 248–254.

[30] Laemmli, U. K., *Nature* 1970, *227*, 680–685.

[31] Ng, M. Y. T., Tan, W. S., Abdullah, N., Ling, T. C., Tey, B. T., *J. Virol. Methods* 2006, *137*, 134–139.

[32] Ferré-D'Amaré, A. R., Burley, S. K., in: Charles W. Carter, Jr. (Eds.), *Methods in Enzymology*, Academic Press, San Diego 1997, pp. 157–166.

[33] Yap, W. B., Tey, B. T., Alitheen, N. B. M., Tan, W. S., *J. Chromatogr. A*. 2010, *1217*, 3473–3480.

[34] Ng, M. Y. T., Tan, W. S., Tey, B. T., *J. Chromatogr. B*. 2012, *903*, 60–67.

[35] Rheinländer, T., Roessner, D., Weitschies, W., Semmler, W., *J. Magn. Magn. Mater*. 2000, *214*, 269–275.

[36] Serwer, P., *J. Ultrastruc. Res*. 1977, *58*, 235–243.

[37] Tan, W. S., McNae, I. W., Ho, K. L., Walkinshaw, M. D., *Acta Crystallogr. F* 2007, *63*, 642–647.

[38] Serwer, P., Khan, S. A., Griess, G. A., *J. Chromatogr. A* 1995, *698*, 251–261.

[39] Griess, G. A., Moreno, E. T., Easom, R. A., Serwer, P., *Biopolymers* 1989, *28*, 1475–1484.

[40] Fang, P.-A., Wright, E. T., Weintraub, S. T., Hakala, K., Wu, W., Serwer, P., Jiang, W., *J. Mol. Biol*. 2008, *384*, 1384–1399.

[41] Neuhoff, V., Arold, N., Taube, D., Ehrhardt, W., *Electrophoresis* 1988, *9*, 255–262.

[42] Serwer, P., Pichler, M. E., *J. Virol*. 1978, *28*, 917–928.

[43] Zlotnick, A., Cheng, N., Conway, J. F., Booy, F. P., Steven, A. C., Stahl, S. J., Wingfield, P. T., *Biochemistry* 1996, *35*, 7412–7421.

[44] Clemmitt, R. H., Chase, H. A., *J. Chromatogr. A* 2000, *874*, 27–43.

